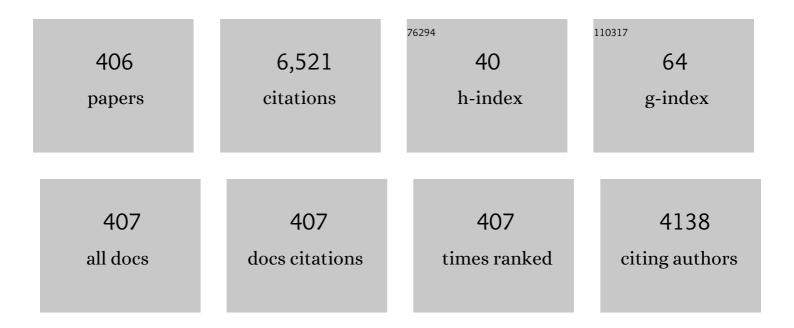
## **Dimitrios Peroulis**

List of Publications by Year in descending order

Source: https://exaly.com/author-pdf/9599044/publications.pdf Version: 2024-02-01



#	Article	IF	CITATIONS
1	Nanohybrids of a MXene and transition metal dichalcogenide for selective detection of volatile organic compounds. Nature Communications, 2020, 11, 1302.	5.8	294
2	Surface Functionalization of Ti <sub>3</sub> C <sub>2</sub> T <sub><i>x</i></sub> MXene with Highly Reliable Superhydrophobic Protection for Volatile Organic Compounds Sensing. ACS Nano, 2020, 14, 11490-11501.	7.3	247
3	A hierarchical manifold microchannel heat sink array for high-heat-flux two-phase cooling of electronics. International Journal of Heat and Mass Transfer, 2018, 117, 319-330.	2.5	231
4	Design of Highly Efficient Broadband Class-E Power Amplifier Using Synthesized Low-Pass Matching Networks. IEEE Transactions on Microwave Theory and Techniques, 2011, 59, 3162-3173.	2.9	224
5	Design of Broadband Highly Efficient Harmonic-Tuned Power Amplifier Using In-Band Continuous Class-\${hbox{F}}^{-1}/{hbox{F}} Mode Transferring. IEEE Transactions on Microwave Theory and Techniques, 2012, 60, 4107-4116.	2.9	179
6	High-\$Q\$ Fully Reconfigurable Tunable Bandpass Filters. IEEE Transactions on Microwave Theory and Techniques, 2009, 57, 3525-3533.	2.9	163
7	High-\$Q\$ Tunable Microwave Cavity Resonators and Filters Using SOI-Based RF MEMS Tuners. Journal of Microelectromechanical Systems, 2010, 19, 774-784.	1.7	156
8	Single/multi-band Wilkinson-type power dividers with embedded transversal filtering sections and application to channelized filters. IEEE Transactions on Circuits and Systems I: Regular Papers, 2015, 62, 1518-1527.	3.5	99
9	Low-frequency meandering piezoelectric vibration energy harvester. IEEE Transactions on Ultrasonics, Ferroelectrics, and Frequency Control, 2012, 59, 846-858.	1.7	94
10	Characterization of hierarchical manifold microchannel heat sink arrays under simultaneous background and hotspot heating conditions. International Journal of Heat and Mass Transfer, 2018, 126, 1289-1301.	2.5	91
11	Highly Loaded Evanescent Cavities for Widely Tunable High-Q Filters. IEEE MTT-S International Microwave Symposium Digest IEEE MTT-S International Microwave Symposium, 2007, , .	0.0	85
12	Theory and Design of Octave Tunable Filters With Lumped Tuning Elements. IEEE Transactions on Microwave Theory and Techniques, 2013, 61, 4353-4364.	2.9	78
13	A Tunable Bandpass-to-Bandstop Reconfigurable Filter With Independent Bandwidths and Tunable Response Shape. IEEE Transactions on Microwave Theory and Techniques, 2010, 58, 3770-3779.	2.9	77
14	Switchless Tunable Bandstop-to-All-Pass Reconfigurable Filter. IEEE Transactions on Microwave Theory and Techniques, 2012, 60, 1258-1265.	2.9	76
15	A Microresonator Design Based on Nonlinear 1 : 2 Internal Resonance in Flexural Structural Modes. Journal of Microelectromechanical Systems, 2009, 18, 744-762.	1.7	75
16	A 6-Gb/s Wireless Inter-Chip Data Link Using 43-GHz Transceivers and Bond-Wire Antennas. IEEE Journal of Solid-State Circuits, 2009, 44, 2711-2721.	3.5	75
17	Co-Design of Highly Efficient Power Amplifier and High-\$Q\$ Output Bandpass Filter. IEEE Transactions on Microwave Theory and Techniques, 2013, 61, 3940-3950.	2.9	72
18	Frequency response of atmospheric pressure gas breakdown in micro/nanogaps. Applied Physics Letters, 2013, 103, .	1.5	61

#	Article	IF	CITATIONS
19	New Bandstop Filter Circuit Topology and Its Application to Design of a Bandstop-to-Bandpass Switchable Filter. IEEE Transactions on Microwave Theory and Techniques, 2013, 61, 1114-1123.	2.9	59
20	Design of Adaptive Highly Efficient GaN Power Amplifier for Octave-Bandwidth Application and Dynamic Load Modulation. IEEE Transactions on Microwave Theory and Techniques, 2012, 60, 1829-1839.	2.9	58
21	Pre-breakdown evaluation of gas discharge mechanisms in microgaps. Applied Physics Letters, 2013, 102,	1.5	56
22	A 3.1-GHz Class-F Power Amplifier With 82% Power-Added-Efficiency. IEEE Microwave and Wireless Components Letters, 2013, 23, 436-438.	2.0	55
23	Hybrid Low-Power Wide-Area Mesh Network for IoT Applications. IEEE Internet of Things Journal, 2021, 8, 901-915.	5.5	54
24	Liquid RF MEMS Wideband Reflective and Absorptive Switches. IEEE Transactions on Microwave Theory and Techniques, 2007, 55, 2919-2929.	2.9	53
25	Multi-Stub-Loaded Differential-Mode Planar Multiband Bandpass Filters. IEEE Transactions on Circuits and Systems II: Express Briefs, 2018, 65, 271-275.	2.2	52
26	Dynamics of a nonlinear microresonator based onÂresonantly interacting flexural-torsional modes. Nonlinear Dynamics, 2008, 54, 31-52.	2.7	50
27	Isolating Bandpass Filters Using Time-Modulated Resonators. IEEE Transactions on Microwave Theory and Techniques, 2019, 67, 2331-2345.	2.9	49
28	DNA counterion current and saturation examined by a MEMS-based solid state nanopore sensor. Biomedical Microdevices, 2006, 8, 263-269.	1.4	48
29	Tunable Inter-Resonator Coupling Structure With Positive and Negative Values and Its Application to the Field-Programmable Filter Array (FPFA). IEEE Transactions on Microwave Theory and Techniques, 2011, 59, 3389-3400.	2.9	47
30	Reconfigurable Single/Multi-Band Filtering Power Divider Based on Quasi-Bandpass Sections. IEEE Microwave and Wireless Components Letters, 2016, 26, 684-686.	2.0	47
31	Tuned to Resonance: Transfer-Function-Adaptive Filters in Evanescent-Mode Cavity-Resonator Technology. IEEE Microwave Magazine, 2014, 15, 55-69.	0.7	46
32	Hybrid Acoustic-Wave-Lumped-Element Resonators (AWLRs) for High- <formula formulatype="inline"&gt;<tex notation="TeX">\$Q\$</tex>  Bandpass Filters With Quasi-Elliptic Frequency Response. IEEE Transactions on Microwave Theory and Techniques, 2015, 63, 2233-2244.</formula 	2.9	44
33	A High-Power Widely Tunable Limiter Utilizing an Evanescent-Mode Cavity Resonator Loaded With a Gas Discharge Tube. IEEE Transactions on Plasma Science, 2016, 44, 3271-3280.	0.6	44
34	Novel Dual-Band Microwave Filter Using Dual-Capacitively-Loaded Cavity Resonators. IEEE Microwave and Wireless Components Letters, 2010, 20, 610-612.	2.0	43
35	Power Handling of Electrostatic MEMS Evanescent-Mode (EVA) Tunable Bandpass Filters. IEEE Transactions on Microwave Theory and Techniques, 2012, 60, 270-283.	2.9	43
36	Quasi-Elliptic Multi-Band Filters With Center-Frequency and Bandwidth Tunability. IEEE Microwave and Wireless Components Letters, 2016, 26, 192-194.	2.0	42

#	Article	IF	CITATIONS
37	Tunable SIW Cavity-Based Dual-Mode Diplexers With Various Single-Ended and Balanced Ports. IEEE Transactions on Microwave Theory and Techniques, 2018, 66, 1238-1248.	2.9	42
38	Bandpass–Bandstop Filter Cascade Performance Over Wide Frequency Tuning Ranges. IEEE Transactions on Microwave Theory and Techniques, 2010, 58, 3945-3953.	2.9	41
39	Co-Design of Multi-Band High-Efficiency Power Amplifier and Three-Pole High-\$Q\$ Tunable Filter. IEEE Microwave and Wireless Components Letters, 2013, 23, 647-649.	2.0	41
40	Extended Passband Bandstop Filter Cascade With Continuous 0.85–6.6-GHz Coverage. IEEE Transactions on Microwave Theory and Techniques, 2012, 60, 21-30.	2.9	40
41	Handling RF Power: The Latest Advances in RF-MEMS Tunable Filters. IEEE Microwave Magazine, 2013, 14, 24-38.	0.7	39
42	Characterizing multi-way interference in wireless mesh networks. , 2006, , .		38
43	Tunable VHF Miniaturized Helical Filters. IEEE Transactions on Microwave Theory and Techniques, 2014, 62, 282-289.	2.9	38
44	Fully-Reconfigurable Bandpass/Bandstop Filters and Their Coupling-Matrix Representation. IEEE Microwave and Wireless Components Letters, 2016, 26, 22-24.	2.0	38
45	High temperature dynamic viscosity sensor for engine oil applications. Sensors and Actuators A: Physical, 2012, 173, 102-107.	2.0	36
46	Fully Adaptive Multiband Bandstop Filtering Sections and Their Application to Multifunctional Components. IEEE Transactions on Microwave Theory and Techniques, 2016, 64, 4405-4418.	2.9	35
47	RF Wide-Band Bandpass Filter With Dynamic In-Band Multi-Interference Suppression Capability. IEEE Transactions on Circuits and Systems II: Express Briefs, 2018, 65, 898-902.	2.2	34
48	Design, Fabrication, and Characterization of a Compact Hierarchical Manifold Microchannel Heat Sink Array for Two-Phase Cooling. IEEE Transactions on Components, Packaging and Manufacturing Technology, 2019, 9, 1291-1300.	1.4	34
49	A Yagi–Uda Array of High-Efficiency Wire-Bond Antennas for On-Chip Radio Applications. IEEE Transactions on Microwave Theory and Techniques, 2009, 57, 3315-3321.	2.9	33
50	Tunable MEMS Spiral Inductors With Optimized RF Performance and Integrated Large-Displacement Electrothermal Actuators. IEEE Transactions on Microwave Theory and Techniques, 2009, 57, 2276-2283.	2.9	32
51	All-Silicon Technology for High-\$Q\$ Evanescent Mode Cavity Tunable Resonators and Filters. Journal of Microelectromechanical Systems, 2014, 23, 727-739.	1.7	31
52	Design and characterization of a low frequency 2-dimensional magnetic levitation kinetic energy harvester. Sensors and Actuators A: Physical, 2015, 236, 1-10.	2.0	31
53	Dispersion Limitations of Ultra-Wideband Wireless Links and Their Compensation Via Photonically Enabled Arbitrary Waveform Generation. IEEE Transactions on Microwave Theory and Techniques, 2008, 56, 710-719.	2.9	30
54	A 3.4 – 6.2 GHz Continuously tunable electrostatic MEMS resonator with quality factor of 460–530. , 2009, , .		30

#	Article	IF	CITATIONS
55	Theory and Design of Frequency-Tunable Absorptive Bandstop Filters. IEEE Transactions on Circuits and Systems I: Regular Papers, 2018, 65, 1862-1874.	3.5	30
56	Intersecting Parallel-Plate Waveguide Loaded Cavities for Dual-Mode and Dual-Band Filters. IEEE Transactions on Microwave Theory and Techniques, 2013, 61, 1829-1838.	2.9	29
57	Design and Optimization of Tunable Silicon-Integrated Evanescent-Mode Bandpass Filters. IEEE Transactions on Microwave Theory and Techniques, 2018, 66, 1790-1803.	2.9	29
58	Tunable Cavity-Based Diplexer With Spectrum-Aware Automatic Tuning. IEEE Transactions on Microwave Theory and Techniques, 2017, 65, 934-944.	2.9	28
59	An Electronically Tunable High-Power Impedance Tuner With Integrated Closed-Loop Control. IEEE Microwave and Wireless Components Letters, 2017, 27, 754-756.	2.0	28
60	Non-Toxic Liquid-Metal 2-100 GHz MEMS Switch. , 2007, , .		27
61	Evaporative intrachip hotspot cooling with a hierarchical manifold microchannel heat sink array. , 2016, , .		27
62	Multilayered Reflectionless Wideband Bandpass Filters With Shunt/In-Series Resistively Terminated Microstrip Lines. IEEE Transactions on Microwave Theory and Techniques, 2020, 68, 877-893.	2.9	27
63	A 6 to 24 GHz continuously tunable, microfabricated, high-Q cavity resonator with electrostatic MEMS actuation. , 2012, , .		26
64	Wireless Temperature Sensor for Condition Monitoring of Bearings Operating Through Thick Metal Plates. IEEE Sensors Journal, 2013, 13, 2292-2298.	2.4	26
65	Plasma-Enabled Tuning of a Resonant RF Circuit. IEEE Transactions on Plasma Science, 2016, 44, 1396-1404.	0.6	26
66	Single and Multiband Acoustic-Wave-Lumped- Element-Resonator (AWLR) Bandpass Filters With Reconfigurable Transfer Function. IEEE Transactions on Microwave Theory and Techniques, 2016, 64, 4394-4404.	2.9	25
67	Highâ€power impedance tuner utilising substrateâ€integrated evanescentâ€mode cavity technology and external linear actuators. IET Microwaves, Antennas and Propagation, 2019, 13, 2067-2072.	0.7	25
68	Early-Warning Wireless Telemeter for Harsh-Environment Bearings. , 2007, , .		24
69	An Experimental and Theoretical Investigation of Creep in Ultrafine Crystalline Nickel RF-MEMS Devices. IEEE Transactions on Microwave Theory and Techniques, 2011, 59, 2655-2664.	2.9	24
70	A Wireless Condition Monitoring System Powered by a Sub-100 \$mu\$W Vibration Energy Harvester. IEEE Transactions on Circuits and Systems I: Regular Papers, 2013, 60, 1082-1093.	3.5	24
71	Microwave Gas Breakdown in Tunable Evanescent-Mode Cavity Resonators. IEEE Microwave and Wireless Components Letters, 2014, 24, 351-353.	2.0	23
72	A Flexible Quadrature Coupler With Reconfigurable Frequency and Coupling Ratio in Switchable Coupling Direction. IEEE Transactions on Microwave Theory and Techniques, 2019, 67, 3391-3402.	2.9	23

#	Article	IF	CITATIONS
73	High-Performance Tunable Narrowband SIW Cavity-Based Quadrature Hybrid Coupler. IEEE Microwave and Wireless Components Letters, 2019, 29, 41-43.	2.0	23
74	Time-Domain Measurement of the Frequency-Dependent Delay of Broadband Antennas. IEEE Transactions on Antennas and Propagation, 2008, 56, 39-47.	3.1	22
75	Antibiased Electrostatic RF MEMS Varactors and Tunable Filters. IEEE Transactions on Microwave Theory and Techniques, 2010, 58, 3971-3981.	2.9	21
76	Tunable high-isolation W-band bandstop filters. , 2015, , .		21
77	High-\$Q\$ Tunable Evanescent-Mode Cavity SIW Resonators and Filters With Contactless Tuners. IEEE Transactions on Microwave Theory and Techniques, 2019, 67, 3661-3672.	2.9	21
78	High-efficiency wire bond antennas for on-chip radios. , 2009, , .		20
79	Energy-Efficient Transmission for Beamforming in Wireless Sensor Networks. , 2010, , .		20
80	Integrated Systems in the More-Than-Moore Era: Designing Low-Cost Energy-Efficient Systems Using Heterogeneous Components. IEEE Design and Test, 2016, 33, 56-65.	1.1	20
81	Fullyâ€ŧunable filtering power dividers exploiting dynamic transmissionâ€zero allocation. IET Microwaves, Antennas and Propagation, 2017, 11, 378-385.	0.7	20
82	Estimating the In-Plane Young's Modulus of Polycrystalline Films in MEMS. Journal of Microelectromechanical Systems, 2012, 21, 840-849.	1.7	19
83	Acoustic-Wave-Lumped-Element-Resonator Filters With Equi-Ripple Absorptive Stopbands. IEEE Microwave and Wireless Components Letters, 2016, 26, 177-179.	2.0	19
84	A Quasi-Absorptive Microwave Resonant Plasma Switch for High-Power Applications. IEEE Transactions on Microwave Theory and Techniques, 2018, 66, 3798-3806.	2.9	19
85	Electrostatic Liquid-Metal Capacitive Shunt MEMS Switch. , 2006, , .		18
86	High-power microwave gas discharge in high-Q evanescent-mode cavity resonators and its instantaneous/long-term effects. , 2013, , .		18
87	Estimating residual stress, curvature and boundary compliance of doubly clamped MEMS from their vibration response. Journal of Micromechanics and Microengineering, 2013, 23, 045009.	1.5	18
88	Octave tunable lumped-element notch filter with resonator-Q-independent zero reflection coefficient. , 2014, , .		18
89	Coupling-Matrix-Based Design of High- <formula formulatype="inline"><tex Notation="TeX"&gt;\$Q\$</tex </formula> Bandpass Filters Using Acoustic-Wave Lumped-Element Resonator (AWLR) Modules. IEEE Transactions on Microwave Theory and Techniques, 2015. 63. 4319-4328.	2.9	18
90	Ultra-Compact Tunable Filtering Rat-Race Coupler Based on Half-Mode SIW Evanescent-Mode Cavity Resonators. IEEE Transactions on Microwave Theory and Techniques, 2018, 66, 5563-5572.	2.9	18

#	Article	IF	CITATIONS
91	Selective Detection of Ethylene by MoS <sub>2</sub> –Carbon Nanotube Networks Coated with Cu(l)–Pincer Complexes. ACS Sensors, 2020, 5, 1699-1706.	4.0	18
92	In-situ control of tunable evanescent-mode cavity filters using differential mode monitoring. , 2009, , .		17
93	Energy efficient collaborative beamforming in wireless sensor networks. , 2009, , .		17
94	Energy-efficient data dissemination using beamforming in wireless sensor networks. ACM Transactions on Sensor Networks, 2013, 9, 1-30.	2.3	17
95	A 23–35 GHz MEMS tunable all-silicon cavity filter with stability characterization up to 140 million cycles. , 2014, , .		17
96	High-Selectivity Tunable Filters With Dual-Mode SIW Resonators in an L-Shaped Coupling Scheme. IEEE Transactions on Microwave Theory and Techniques, 2019, 67, 5016-5028.	2.9	17
97	Context-Aware Collaborative Intelligence With Spatio-Temporal In-Sensor-Analytics for Efficient Communication in a Large-Area IoT Testbed. IEEE Internet of Things Journal, 2021, 8, 6800-6814.	5.5	17
98	A capacitively-loaded MEMS Slot element for wireless temperature sensing of up to 300°C. , 2009, , .		16
99	Tunable bandstop filter with a 17-to-1 upper passband. , 2012, , .		16
100	Real-Time Feedback Control System for Tuning Evanescent-Mode Cavity Filters. IEEE Transactions on Microwave Theory and Techniques, 2016, 64, 2804-2813.	2.9	16
101	Tunable Constant-Bandwidth Substrate-Integrated Bandstop Filters. IEEE Transactions on Microwave Theory and Techniques, 2018, 66, 157-169.	2.9	16
102	Mixed Lumped and Distributed Circuits in Wideband Bandpass Filter Application for Spurious-Response Suppression. IEEE Microwave and Wireless Components Letters, 2018, 28, 978-980.	2.0	16
103	Multifunctional Bandpass Filters With Reconfigurable and Switchable Band Control. IEEE Transactions on Microwave Theory and Techniques, 2019, 67, 2355-2369.	2.9	16
104	Time-Varying Matching Networks for Signal-Centric Systems. IEEE Transactions on Microwave Theory and Techniques, 2007, 55, 2599-2613.	2.9	15
105	Contribution of ions in radio frequency properties of atmospheric pressure microgaps. Applied Physics Letters, 2014, 105, .	1.5	15
106	Series-cascaded absorptive notch-filters for 4G-LTE radios. , 2015, , .		15
107	Reconfigurable Multiband Bandpass Filters in Evanescent-Mode-Cavity-Resonator Technology. IEEE Microwave and Wireless Components Letters, 2017, 27, 248-250.	2.0	15

Silicon Micromachined Packages for RF MEMS Switches. , 2001, , .

#	Article	IF	CITATIONS
109	A viscoelastic-aware experimentally-derived model for analog RF MEMS varactors. , 2010, , .		14
110	Power handling of high-Q evanescent-mode tunable filter with integrated piezoelectric actuators. , 2012, , .		14
111	Millimeterâ€wave phase shifter based on waveguideâ€mounted RFâ€MEMS. Microwave and Optical Technology Letters, 2013, 55, 465-468.	0.9	14
112	Acoustic Wave Resonator-Based Absorptive Bandstop Filters With Ultra-Narrow Bandwidth. IEEE Microwave and Wireless Components Letters, 2015, 25, 570-572.	2.0	14
113	High- <inline-formula> <tex-math notation="LaTeX"&gt;\$Q\$</tex-math </inline-formula> Bandstop Filters Exploiting Acoustic-Wave-Lumped-Element Resonators (AWLRs). IEEE Transactions on Circuits and Systems II: Express Briefs, 2016, 63, 79-83.	2.2	14
114	Tune-All RF Planar Duplexers With Intrinsically Switched Channels. IEEE Microwave and Wireless Components Letters, 2017, 27, 350-352.	2.0	14
115	A widely-tunable substrate-integrated balun filter. , 2017, , .		14
116	An inherently-robust 300°C MEMS temperature sensor for wireless health monitoring of ball and rolling element bearings. , 2009, , .		13
117	Thermal and Electrical Conductivities of Nanocrystalline Nickel Microbridges. Journal of Microelectromechanical Systems, 2012, 21, 850-858.	1.7	13
118	A novel high-Q <inf>u</inf> octave-tunable resonator with lumped tuning elements. , 2013, , .		13
119	High-Q intrinsically-switched quasi-absorptive tunable bandstop filter with electrically-short resonators. , 2014, , .		13
120	Highly Linear and Highly Efficient Dual-Carrier Power Amplifier Based on Low-Loss RF Carrier Combiner. IEEE Transactions on Microwave Theory and Techniques, 2014, 62, 590-599.	2.9	13
121	Dynamic Bandpass Filter Shape and Interference Cancellation Control Utilizing Bandpass–Bandstop Filter Cascade. IEEE Transactions on Microwave Theory and Techniques, 2015, 63, 2526-2539.	2.9	13
122	A class of fully-reconfigurable planar multi-band bandstop filters. , 2016, , .		13
123	Low-pressure gas sensor exploiting the Knudsen thermal force: DSMC modeling and experimental validation. , 2016, , .		13
124	Wide-passband filters with in-band tunable notches for agile multi-interference suppression in broad-band antenna systems. , 2018, , .		13
125	Planar Multifrequency Wideband Bandpass Filters With Constant and Frequency Mappings. IEEE Transactions on Microwave Theory and Techniques, 2018, 66, 935-942.	2.9	13
126	A Novel Independently-Tunable Dual-Mode SIW Resonator with a Reconfigurable Bandpass Filter Application. , 2018, , .		13

#	Article	IF	CITATIONS
127	Fast Frequency-Agile Real-Time Optimization of High-Power Tuning Network for Cognitive Radar Applications. , 2019, , .		13
128	A Flexible Virtual Battery: A Wearable Wireless Energy Harvester. IEEE Microwave Magazine, 2019, 20, 62-69.	0.7	13
129	Fast Optimization Algorithm for Evanescent-Mode Cavity Tuner Optimization and Timing Reduction in Software-Defined Radar Implementation. IEEE Transactions on Aerospace and Electronic Systems, 2020, 56, 2762-2778.	2.6	13
130	On-chip bond-wire antennas on CMOS-grade silicon substrates. , 2008, , .		12
131	A single-crystal silicon DC-40 GHz RF MEMS switch. , 2009, , .		12
132	High Q narrow-band tunable filters with controllable bandwidth. , 2009, , .		12
133	Tunable, substrate integrated, high Q filter cascade for high isolation. , 2010, , .		12
134	Impact of Mechanical Vibration on the Performance of RF MEMS Evanescent-Mode Tunable Resonators. IEEE Microwave and Wireless Components Letters, 2011, 21, 406-408.	2.0	12
135	Direct measurement of field emission current in E-static MEMS structures. , 2011, , .		12
136	Low-Order Filter Response Enhancement in Reconfigurable Resonator Arrays. IEEE Transactions on Microwave Theory and Techniques, 2013, 61, 4387-4395.	2.9	12
137	A Tunable Miniaturized RF MEMS Resonator With Simultaneous High ⁢formula formulatype="inline"> <tex notation="TeX">\$Q\$</tex> (500–735) and Fast Response Speed <formula formulatype="inline"><tex Notation="TeX"&gt;\$(<hbox{10}-hbox{60} muhbox{s})\$<="" tex=""></hbox{10}-hbox{60}></tex </formula> . Journal	1.7	12
138	Vâ€band bandpass filter with continuously variable centre frequency. IET Microwaves, Antennas and Propagation, 2013, 7, 701-707.	0.7	12
139	A Compact L-Band Bandpass Filter with RF MEMS-Enabled Reconfigurable Notches for Interference Rejection in GPS Applications. IEEE Microwave Magazine, 2015, 16, 81-88.	0.7	12
140	A PCB Technology-Based 22–42-CHz Quasi-Absorptive Bandstop Filter. IEEE Microwave and Wireless Components Letters, 2018, 28, 975-977.	2.0	12
141	A Wearable Real-Time CMOS Dosimeter With Integrated Zero-Bias Floating Gate Sensor and an 861-nW 18-Bit Energy-Resolution Scalable Time-Based Radiation to Digital Converter. IEEE Journal of Solid-State Circuits, 2020, 55, 650-665.	3.5	12
142	Bandpass Filter With Tunable/Switchable In-Band Interference Rejection. IEEE Microwave and Wireless Components Letters, 2021, 31, 1115-1118.	2.0	12
143	A Fiber-Free DC-7 GHz 35 W Integrated Semiconductor Plasma Switch. , 2021, , .		12

An Evanescent-mode Cavity Resonator Based Thermal Sensor. , 2007, , .

#	Article	IF	CITATIONS
145	Radiating sensor selection for distributed beamforming in wireless sensor networks. , 2008, , .		11
146	A Phenomenological Discrete Brittle Damage-Mechanics Model for Fatigue of MEMS Devices With Application to LIGA Ni. Journal of Microelectromechanical Systems, 2009, 18, 119-128.	1.7	11
147	A 12–18 GHz electrostatically tunable liquid metal RF MEMS resonator with quality factor of 1400–1840. , 2011, , .		11
148	A CAD Model for Creep Behavior of RF-MEMS Varactors and Circuits. IEEE Transactions on Microwave Theory and Techniques, 2011, 59, 1761-1768.	2.9	11
149	Uncertainty in microscale gas damping: Implications on dynamics of capacitive MEMS switches. Reliability Engineering and System Safety, 2011, 96, 1171-1183.	5.1	11
150	Widely Tunable High-Efficiency Power Amplifier With Ultra-Narrow Instantaneous Bandwidth. IEEE Transactions on Microwave Theory and Techniques, 2012, 60, 3787-3797.	2.9	11
151	Wide spurious free range positive-to-negative inter-resonator coupling structure for reconfigurable filters. , 2013, , .		11
152	Multiple Timescales and Modeling of Dynamic Bounce Phenomena in RF MEMS Switches. Journal of Microelectromechanical Systems, 2014, 23, 137-146.	1.7	11
153	A 20–40 GHz tunable MEMS bandpass filter with enhanced stability by gold-vanadium micro-corrugated diaphragms. , 2016, , .		11
154	Signal-interference bandpass filters with dynamic in-band interference suppression. , 2016, , .		11
155	Recent advances in reconfigurable microwave filter design. , 2016, , .		11
156	Wireless Sensor Network Utilizing Flexible Nitrate Sensors for Smart Farming. , 2019, , .		11
157	Alleviating the Adverse Effects of Residual Stress in RF MEMS Switches. , 2001, , .		10
158	Cyclic evolution of bouncing for contacts in commercial RF MEMS switches. , 2012, , .		10
159	Reconfigurable bandpass filter with center frequency and bandwidth control. Microwave and Optical Technology Letters, 2013, 55, 2745-2750.	0.9	10
160	High-Q MEMS-tunable W-band bandstop resonators. , 2014, , .		10
161	Transformers with incorporated filtering capabilities exploiting signal-interference principles. , 2015, , .		10
162	A VHF tunable lumped-element filter with mixed electric-magnetic couplings. , 2015, , .		10

#	Article	IF	CITATIONS
163	Time-varying matching network for antennas in pulse-based systems. , 2007, , .		9
164	Low-Cost 3-D Integration of RF and Micro-Cooling Systems. , 2008, , .		9
165	Tunable high Q narrow-band triplexer. , 2009, , .		9
166	RF Design, Power Handling, and Hot Switching of Waveguide Water-Based Absorptive Switches. IEEE Transactions on Microwave Theory and Techniques, 2009, 57, 2038-2046.	2.9	9
167	Reconfigurable-order bandpass filter for frequency agile systems. , 2010, , .		9
168	A wireless sensor node for condition monitoring powered by a vibration energy harvester. , 2011, , .		9
169	High-Q tunable bandstop filters with adaptable bandwidth and pole allocation. , 2011, , .		9
170	Design of broadband high-efficiency power amplifier using in-band Class-F <sup>−1</sup> /F mode-transferring technique. , 2012, , .		9
171	An Analytical Capacitance Model of Temperature-Sensitive, Large-Displacement Multimorph Cantilevers: Numerical and Experimental Validation. Journal of Microelectromechanical Systems, 2012, 21, 161-170.	1.7	9
172	Vibration mitigation for evanescent-mode cavity filters. , 2014, , .		9
173	Dark-to-arc transition in field emission dominated atmospheric microdischarges. Physics of Plasmas, 2015, 22, .	0.7	9
174	Hybrid surfaceâ€acousticâ€wave/microstrip signalâ€interference bandpass filters. IET Microwaves, Antennas and Propagation, 2016, 10, 426-434.	0.7	9
175	Design of an airline coax radial power combiner with enhanced isolation. , 2017, , .		9
176	Frequency-Selective Limiters Using Triple-Mode Filters. IEEE Access, 2020, 8, 114854-114863.	2.6	9
177	A high-efficiency low-cost wire-bond loop antenna for CMOS wafers. Digest / IEEE Antennas and Propagation Society International Symposium, 2009, , .	0.0	8
178	Non-toxic liquid metal microstrip resonators. , 2009, , .		8
179	Analysis and Measurement of a Time-Varying Matching Scheme for Pulse-Based Receivers With High-\$Q\$ Sources. IEEE Transactions on Microwave Theory and Techniques, 2010, 58, 2231-2243.	2.9	8
180	Arrays of silicon cantilevers for detecting high-G rapidly varying acceleration profiles. , 2010, , .		8

#	Article	IF	CITATIONS
181	Wireless Temperature Sensor Operating in Complete Metallic Environment Using Permanent Magnets. IEEE Transactions on Magnetics, 2012, 48, 4413-4416.	1.2	8
182	Highly Reliable MEMS Temperature Sensors for 275 \$^{ circ}hbox{C}\$ Applications—Part 2: Creep and Cycling Performance. Journal of Microelectromechanical Systems, 2013, 22, 236-243.	1.7	8
183	Near-Contact Gas Damping and Dynamic Response of High-g MEMS Accelerometer Beams. Journal of Microelectromechanical Systems, 2013, 22, 1089-1099.	1.7	8
184	A class of planar multi-band Wilkinson-type power divider with intrinsic filtering functionality. , 2015, , .		8
185	An Adaptive Educational Web Application for Engineering Students. IEEE Access, 2017, 5, 359-365.	2.6	8
186	SAW-based bandpass filters with flat in-band group delay and enhanced fractional bandwidth. , 2017, , .		8
187	Constant In-Band Group-Delay Acoustic-Wave-Lumped-Element-Resonator-Based Bandpass Filters and Diplexers. IEEE Transactions on Microwave Theory and Techniques, 2018, 66, 2199-2209.	2.9	8
188	Monitoring and Control of MEMS Tunable Filters Using Inductive Proximity Sensing. IEEE Transactions on Microwave Theory and Techniques, 2018, 66, 5605-5613.	2.9	8
189	Balanced octave-tunable absorptive bandstop filter. , 2018, , .		8
190	A 20–26.5-GHz PCB Bandpass Filter Tuned With Contactless Tuners. IEEE Microwave and Wireless Components Letters, 2019, 29, 513-515.	2.0	8
191	A Photogenerated Silicon Plasma Waveguide Switch and Variable Attenuator for Millimeter-Wave Applications. IEEE Transactions on Microwave Theory and Techniques, 2021, 69, 5393-5403.	2.9	8
192	Power handling capability of High-Q evanescent-mode RF MEMS resonators with flexible diaphragm. , 2009, , .		7
193	Vibration-Based Monitoring and Diagnosis of Dielectric Charging in RF-MEMS Switches. Journal of Microelectromechanical Systems, 2010, 19, 1490-1502.	1.7	7
194	Adaptive-transfer-function bandpass filters using reconfigurable evanescent-mode-cavity resonator cascades. , 2016, , .		7
195	Temperature-compensated lumped element tunable bandpass filter. , 2016, , .		7
196	Octave-tunable constant absolute bandwidth bandstop filter utilizing a novel passively-compensated coupling method. , 2016, , .		7
197	Design and implementation of an intrinsically-switched 22–43 GHz tunable bandstop filter. , 2016, , .		7
198	3D MOS-capacitor-based ionizing radiation sensors. , 2017, , .		7

3D MOS-capacitor-based ionizing radiation sensors. , 2017, , . 198

#	Article	IF	CITATIONS
199	A Compact Tunable Filtering Rat-Race Coupler. , 2018, , .		7
200	Hybrid Bandpass-Absorptive-Bandstop Magnetically Coupled Acoustic-Wave-Lumped-Element-Resonator Filters. IEEE Microwave and Wireless Components Letters, 2018, 28, 582-584.	2.0	7
201	An Evanescent-Mode Cavity-Backed High-Power Tunable Slot Antenna. IEEE Transactions on Antennas and Propagation, 2019, 67, 3712-3719.	3.1	7
202	A Plasma-Switch Impedance Tuner for Real-Time, Frequency-Agile, High-Power Radar Transmitter Reconfiguration. , 2021, , .		7
203	K-band loss characterization of electroplated nickel for RF MEMS devices. , 2007, , .		6
204	Impact of sacrificial layer type on thin-film metal residual stress. , 2009, , .		6
205	Real-time monitoring of contact behavior of RF MEMS switches with a very low power CMOS capacitive sensor interface. , 2010, , .		6
206	A high-Q magnetostatically-tunable all-silicon evanescent cavity resonator. , 2011, , .		6
207	RF-MEMS enabled power divider with arbitrary power division ratio. , 2012, , .		6
208	Wireless temperature sensor for mechanical face seals using permanent magnets. Sensors and Actuators A: Physical, 2013, 203, 369-372.	2.0	6
209	Wireless temperature and vibration sensor for real-time bearing condition monitoring. , 2013, , .		6
210	Analog signal-interference narrow-band bandpass filters with hybrid transmission-line/SAW-resonator transversal filtering sections. , 2015, , .		6
211	A 2–30 W 5-band plasma-based switch. , 2017, , .		6
212	Tunable absorptive bandstop filter with an ultra-broad upper passband. , 2017, , .		6
213	Dual-passband filters and extended-stopband wide-band bandpass filters based on generalized stub-loaded planar circuits. , 2017, , .		6
214	An L-Band Low Phase Noise Evanescent-Mode Cavity-Based Frequency Synthesizer. IEEE Transactions on Circuits and Systems I: Regular Papers, 2018, 65, 2161-2168.	3.5	6
215	Multi-Point Wireless Temperature Sensing System for Monitoring Pharmaceutical Lyophilization. Frontiers in Chemistry, 2018, 6, 288.	1.8	6
216	Fast impedance matching using interval halving of resonator position numbers for a high-power evanescent-mode cavity tuner. , 2018, , .		6

#	Article	IF	CITATIONS
217	Design and Optimization of Bidirectional Tunable MEMS All-Silicon Evanescent-Mode Cavity Filter. IEEE Transactions on Microwave Theory and Techniques, 2020, 68, 2398-2408.	2.9	6
218	A non-invasive multipoint product temperature measurement for pharmaceutical lyophilization. Scientific Reports, 2022, 12, .	1.6	6
219	Time-Domain Impedance Adaptors for Pulse-Based Systems with High Q RC loads. IEEE MTT-S International Microwave Symposium Digest IEEE MTT-S International Microwave Symposium, 2007, , .	0.0	5
220	Fully electronic method for quantifying the post-release gap-height uncertainty of capacitive RF MEMS switches. , 2009, , .		5
221	An experimental investigation on viscoelastic behavior in tunable planar RF-MEMS resonators. , 2010, , $\cdot$		5
222	Analysis of Energy Consumption on Data Sharing in Beamforming for Wireless Sensor Networks. , 2010, , .		5
223	Bandwidth-optimal single-tunable-element matching network for antenna tuning in mobile handsets. , 2011, , .		5
224	Co-design of power amplifier and narrowband filter using high-Q evanescent-mode cavity resonator as the output matching network. , 2011, , .		5
225	A fast high-Q X-band RF-MEMS reconfigurable evanescent-mode cavity resonator. , 2012, , .		5
226	Non-linear effects in MEMS tunable bandstop filters. , 2012, , .		5
227	A polarization-reconfigurable filtering antenna system: a visual approach to investigating the bandwidth of transmission lines with non-z0 impedance [education column]. IEEE Antennas and Propagation Magazine, 2013, 55, 197-235.	1.2	5
228	Significance of Adhesion-Reduced Bouncing in Dynamic Contacts of Ohmic RF MEMS Switches. Journal of Microelectromechanical Systems, 2015, 24, 1487-1494.	1.7	5
229	Bandwidth enlargement in acoustic-wave RF bandpass filters with planar transversal circuits. , 2015, , .		5
230	An equation-based nonlinear model for non-flat MEMS fixed–fixed beams with non-vertical anchoring supports. Journal of Micromechanics and Microengineering, 2015, 25, 055018.	1.5	5
231	Advances in high-Q tunable filter technologies. International Journal of Advances in Engineering Sciences and Applied Mathematics, 2015, 7, 170-176.	0.7	5
232	RF-design of narrowband absorptive bandstop filters for UHF applications. , 2015, , .		5
233	Spectrum-aware jammer suppression using evanescent-mode cavity filters. , 2015, , .		5
234	Tunable acoustic-wave-lumped-element resonator (awlr)-based bandpass filters. , 2016, , .		5

234 Tunable acoustic-wave-lumped-element resonator (awlr)-based bandpass filters. , 2016, , .

4

#	Article	IF	CITATIONS
235	A class of differential-mode single/dual-band bandpass planar filters based on signal-interference techniques. , 2016, , .		5
236	Gas discharge tube-based variable RF attenuator. , 2016, , .		5
237	A tunable 0.86–1.03 GHz FDD wireless communication system with an evanescent-mode diplexer and a self-interference-cancelling receiver. , 2017, , .		5
238	High-Power Wideband Low-Cost Limiters Using Cold Plasma. , 2018, , .		5
239	Mid-Range Wireless Power Transfer Based on Goubau Lines. , 2018, , .		5
240	Reflectionless Wideband Bandpass Filter Designed With Multilayered Microstrip Vertical Transition. , 2019, , .		5
241	Plasma Switch-Based Technology for High-Speed and High-Power Impedance Tuning. , 2021, , .		5
242	Dual-Band Dual-Mode Filter-Enhanced Linearity Measurement. IEEE Microwave and Wireless Components Letters, 2021, 31, 1083-1085.	2.0	5
243	High-Q High Power Tunable Filters Manufactured With Injection Molding Technology. IEEE Access, 2022, 10, 19643-19653.	2.6	5
244	RF MEMS switches for leakage control in wireless handheld devices. , 2007, , .		4
245	Bearing cage telemeter for the detection of shaft imbalance in rotating systems. , 2010, , .		4
246	System-level characterization of bias noise effects on electrostatic RF MEMS tunable filters. , 2011, , .		4
247	MEMS-Based Power Gating for Highly Scalable Periodic and Event-Driven Processing. , 2011, , .		4
248	Tunable bandpass and bandstop filter cascade for dynamic pole allocation. , 2012, , .		4
249	Wireless chip-to-chip communication in three-dimensional integrated circuits using microbump antennas. , 2013, , .		4
250	Nano-plasma tunable evanescent-mode cavity resonators. , 2014, , .		4
251	MOS-capacitor-based ionizing radiation sensors for occupational dosimetry applications. , 2015, , .		4

252 Silicon-micromachined spacers for UHF cavity resonators. , 2015, , .

#	Article	IF	CITATIONS
253	Wireless low-power temperature probes for food/pharmaceutical process monitoring. , 2015, , .		4
254	Miniaturized signal-interference planar filters. , 2015, , .		4
255	Design of high-Q absorptive bandstop filters with static and reconfigurable attenuation. , 2015, , .		4
256	Wearable, wireless sensor platform for occupational radiation dosimetry applications. , 2015, , .		4
257	Characterization of fading of a MOS-based sensor for occupational radiation dosimetry. , 2016, , .		4
258	Power limiting characteristics of a plasma-loaded evanescent-mode cavity resonator. , 2016, , .		4
259	V-band frequency reconfigurable cavity-based bandpass filters. , 2016, , .		4
260	Reconfigurable single/multi-band planar impedance transformers with incorporated bandpass filtering functionality. , 2016, , .		4
261	Single/multi-band multi-functional passive components with reconfiguration capabilities. , 2017, , .		4
262	RF design of acoustic-wave-lumped-element-resonator-(AWLR)-based bandpass filters with constant in-band group delay. , 2017, , .		4
263	An S-band 3-W load-reconfigurable power amplifier with 50–76% efficiency for VSWR up to 4:1. , 2017, , .		4
264	Multi-resonant acoustic-wave-lumped-element resonators (AWLRs) for multi-band bandpass filters with enhanced fractional bandwidth. , 2017, , .		4
265	Tunable Filter Technologies for 5G Communications. , 2018, , .		4
266	A Wearable Real-time CMOS Dosimeter with Integrated Zero-bias Floating-Gate Sensor and an 861nW 18-bit Energy-Resolution Scalable Time-based Radiation to Digital Converter. , 2019, , .		4
267	A Programmable Bandpass Filter With Simultaneously Reconfigurable Working Frequency and Bandwidth. , 2019, , .		4
268	Instinctual Interference-Adaptive Low-Power Receiver With Combined Feedforward and Feedback Control. IEEE Microwave and Wireless Components Letters, 2021, 31, 771-774.	2.0	4
269	Statistical electromagnetics for industrial pharmaceutical lyophilization. , 2022, 1, .		4
270	Time-varying matching for receiving wideband pulse through electrically small antennas. , 2008, , .		3

#	Article	IF	CITATIONS
271	Nano-switch for study of gold contact behavior. , 2009, , .		3
272	Three-Bit and Six-Bit Tunable Matching Networks with Tapered Lines. , 2009, , .		3
273	Electrostatically tunable analog single crystal silicon fringing-field MEMS varactors. , 2009, , .		3
274	Phase difference and frequency offset estimation for collaborative beamforming in sensor networks. , 2010, , .		3
275	Anti-biased RF MEMS varactor topology for 20–25 dB linearity enhancement. , 2010, , .		3
276	A monolithic RF-MEMS filter with continuously-tunable center-frequency and bandwidth. , 2011, , .		3
277	<i>In situ</i> monitoring of dynamic bounce phenomena in RF MEMS switches. Journal of Micromechanics and Microengineering, 2013, 23, 115007.	1.5	3
278	Continuously variable W-band phase shifters based on MEMS-actuated conductive fingers. International Journal of Microwave and Wireless Technologies, 2013, 5, 477-489.	1.5	3
279	Implementing wireless communication links in 3-D ICs utilizing wide-band on-chip meandering microbump antenna. , 2013, , .		3
280	Coupling-matrix-based SAW filter design. , 2014, , .		3
281	Measuring Effective Flexure Width by Measuring Comb Drive Capacitance. Journal of Microelectromechanical Systems, 2014, 23, 972-979.	1.7	3
282	Creep-resistant nanocrystalline gold-vanadium alloyed microcorrugated diaphragms (MCDS). , 2015, , .		3
283	Acoustic-wave-lumped-element resonator (AWLR) architectures for high-Q reflective bandstop filters. , 2015, , .		3
284	Variable-output charge-pump for piezoelectric and electrostatic tunable RF filters. , 2015, , .		3
285	Residual Stress Extraction of Surface-Micromachined Fixed-Fixed Nickel Beams Using a Wafer-Scale Technique. Journal of Microelectromechanical Systems, 2015, 24, 1803-1816.	1.7	3
286	Sharp-rejection highpass and dual-band bandpass planar filters with multi-transmission-zero-generation transversal cell. , 2015, , .		3
287	High-Q bandpass filters using hybrid acoustic-wave-lumped-element resonators (AWLRs) for UHF applications. , 2015, , .		3

288 Low temperature plasma for tunable resonant attenuation. , 2016, , .

#	Article	IF	CITATIONS
289	Substrate-integrated-waveguide signal-interference bandpass filters. , 2016, , .		3
290	Continuously-tunable-bandwidth acoustic-wave resonator-based bandstop filters and their multi-mode modeling. , 2016, , .		3
291	An ANT-based low-power battery-free wireless cryogenic temperature probes for industrial process monitoring. , 2016, , .		3
292	Authors' Reply to "Comments on â€~Design of Highly Efficient Broadband Class-E Power Amplifier Using Synthesized Low-Pass Matching Networksâ€â€™. IEEE Transactions on Microwave Theory and Techniques, 2016, 64, 1679-1679.	2.9	3
293	Tunable bandpass-bandstop filter cascade for VHF applications. , 2016, , .		3
294	A 12â $\in$ "20 GHz Passively-compensated Tunable Bandstop Filter with 40-dB Notch Level. , 2018, , .		3
295	Simultaneous analog tuning of the series- and anti-resonances of acoustic wave resonators. , 2018, , .		3
296	A 2.2–4.2 GHz low-loss tunable bandpass filter based on low cost manufacturing of ABS polymer. , 2018, , .		3
297	A New Wireless Power Transmission (WPT) System for Powering Wireless Sensor Networks (WSNs) in Cavity-Based Equipment. , 2019, , .		3
298	A 2.2 – 3.4 GHz Constant Bandwidth High-Selectivity Tunable Filter Based on Dual-Mode SIW Resonators. , 2019, , .		3
299	A Hybrid Low-Cost Bandpass Filter With SAW Resonators and External Lumped Inductors Using a Dual-Coupling Scheme. IEEE Transactions on Microwave Theory and Techniques, 2020, 68, 2289-2299.	2.9	3
300	2–8 GHz Interference Detector With 1.1 μs Response. IEEE Microwave and Wireless Components Letters, 2022, 32, 756-759.	2.0	3
301	Photonically-Synthesized Waveforms to Combat Broadband Antenna Phase Distortions. , 2007, , .		2
302	Nonlinear Resonator With Interacting Flexural-Torsional Modes for Mass Sensing. , 2007, , 967.		2
303	Integrated Inductor Actively Engaging Metal Filling Rules. , 2007, , .		2
304	Loss optimization of coplanar strips for CMOS RFICs. , 2009, , .		2
305	A Micromachined High-Q Microstrip Line with a Broadband Microstrip-to-CPW Transistion. , 2009, , .		2
306	Bandwidth-optimal single shunt-capacitor matching networks for parallel RC loads of Q ≫ 1. , 2009, , .		2

#	Article	IF	CITATIONS
307	Near-contact damping model and dynamic response of. , 2011, , .		2
308	Uncertainty Quantification of Pull-In Phenomenon in Capacitive RF-MEMS. , 2011, , .		2
309	Frequency-agile field-programmable filter array (FPFA) with multiple functionalities. , 2011, , .		2
310	Wireless temperature sensor for condition monitoring of mechanical seals. , 2012, , .		2
311	Highly Reliable MEMS Temperature Sensors for 275 \$^{ circ}hbox{C}\$ Applications—Part 1: Design and Technology. Journal of Microelectromechanical Systems, 2013, 22, 225-235.	1.7	2
312	A wideband 0.7–2.2 GHz tunable power amplifier with over 64% efficiency based on high-Q second harmonic loading. , 2013, , .		2
313	Application of ball bearing cage RF temperature sensor in high speed turbocharger. , 2014, , .		2
314	Thermally Stable Nonuniform Microcorrugated Capacitive MEMS Tuner. Journal of Microelectromechanical Systems, 2015, 24, 522-524.	1.7	2
315	Field emission mitigation in X-band silicon-etched cavity resonators. , 2016, , .		2
316	A tunable VHF gas discharge tube resonator. , 2016, , .		2
317	Electrical properties of creep-resistant nanocrystalline gold-vanadium thin films at millimeter-wave frequencies. , 2016, , .		2
318	Multi-functional low-pass filters with dynamically-controlled in-band rejection notches. , 2016, , .		2
319	A High-Performance Pathway: a 0.95/2.45-GHZ Switched-Frequency Bandpass Filter Using Commercially Available RF MEMS Tuning Elements. IEEE Microwave Magazine, 2016, 17, 34-41.	0.7	2
320	A substrate-integrated-waveguide dual-band bandpass filter based on signal-interference principles. , 2017, , .		2
321	Fast amplifier PAE optimization using resonant frequency interval halving with an evanescent-mode cavity tuner. , 2017, , .		2
322	A 19–40 GHz bi-directional MEMS tunable all silicon evanescent-mode cavity filter. , 2017, , .		2
323	A hybrid, networked, wireless system for humidity sensing. , 2017, , .		2
324	Interaction of high-power microwaves with low-temperature plasma in a gas-discharge-tube-loaded SIW structure. , 2018, , .		2

#	Article	IF	CITATIONS
325	A New Adaptive Reconfigurable Bandpass Filter with Flexible Resonance Control. , 2018, , .		2
326	Real-Time Frequency-Agile \$mathrm{Circuit}\$ Reconfiguration for S-Band Radar Using a High-Power Tunable Resonant Cavity Matching Network. , 2018, , .		2
327	Realâ€time temperature compensation for tunable cavityâ€based BPFs and BSFs. IET Circuits, Devices and Systems, 2018, 12, 785-791.	0.9	2
328	Reconfigurable and Adaptive Radar Amplifiers for Spectrum Sharing in Cognitive Radar. , 2019, , .		2
329	Toward a High-Power High-Isolation Wideband Plasma Limiter. , 2019, , .		2
330	Electrically-Coupled Goubau-Line-Based Wireless Power Transfer System. IEEE Access, 2019, 7, 115886-115900.	2.6	2
331	Balanced-Balanced Tunable Filtering LNA using Evanescent-Mode Resonators. , 2019, , .		2
332	Plasma-Based Power Limitation for Highly Linear MEMS Switch Protection and Isolation Enhancement. IEEE Access, 2020, 8, 173103-173111.	2.6	2
333	A Compact Octave Tunable Switched-Power-Combining PA. IEEE Access, 2021, 9, 15212-15220.	2.6	2
334	Design and Analysis of a Resistive Sensor Interface With Phase Noise-Energy-Resolution Scalability for a Time-Based Resistance-to-Digital Converter. Frontiers in Electronics, 2022, 3, .	2.0	2
335	Spring-loaded DC-contact RF MEMS switches. International Journal of RF and Microwave Computer-Aided Engineering, 2004, 14, 345-355.	0.8	1
336	Hydrogel-Based Integrated Antenna-pH Sensor. , 2007, , .		1
337	A Ka-band waveguide water-based absorptive switch with an integrated micropump. , 2008, , .		1
338	A time-varying matching scheme for pulse-based high-Q receivers. , 2009, , .		1
339	Experimental quantification of temperature uncertainty for an array of thermally-sensitive MEMS cantilever beams. , 2009, , .		1
340	CMOS-based monitoring of contact events up to 4 MHz in ohmic RF MEMS switches. , 2010, , .		1
341	A two-dimensional electronically-steerable array antenna for target detection on ground. , 2011, , .		1
342	Signal-to-Noise Ratio Performance of a Time-Varying Matching Network for Pulse-Based Systems. IEEE Transactions on Microwave Theory and Techniques, 2011, 59, 323-337.	2.9	1

#	Article	IF	CITATIONS
343	Collaborative beamforming in wireless sensor networks. , 2011, , .		1
344	Wideband diode-based reconfigurable matching network operating at 36 dBm input power. , 2012, , .		1
345	Lifetime effects of drive voltage for a commercially-available ohmic-contact RF MEMS switch. , 2013, , .		1
346	A visual approach to investigating the bandwidth of transmission lines with non-Z <sub>O</sub> impedance. IEEE Antennas and Propagation Magazine, 2013, 55, 220-235.	1.2	1
347	Real-Time DC-dynamic Biasing Method for Switching Time Improvement in Severely Underdamped Fringing-field Electrostatic MEMS Actuators. Journal of Visualized Experiments, 2014, , e51251.	0.2	1
348	Real-time temperature compensation control system for tunable cavity-based high-Q filters. , 2015, , .		1
349	A single crystal silicon low-g switch tolerant to impact accelerations up to 24,000 g. , 2015, , .		1
350	A continuously tunable 95â $\in$ "138 MHz bandpass resonator with 40 dBm IIP3. , 2015, , .		1
351	Tuning limits of shunt varactor diodes for maintaining high OIP <inf>3</inf> in arbitrary circuits. , 2015, , .		1
352	Evanescent-mode cavity-based frequency synthesizer. , 2016, , .		1
353	MEMS-tunable silicon-integrated cavity filters. , 2016, , .		1
354	Multi-band signal-interference planar bandpass filters based on stub-loaded transversal filtering sections. , 2016, , .		1
355	A constant-transfer-function widely-tunable VHF modular field-programmable filter array (FPFA) with IIP3 of 38–52 dBm. , 2016, , .		1
356	A high-Q octave-tunable all-silicon cavity filter using magnetostatic actuation. , 2016, , .		1
357	Digital representation of multi-functional microwave passive circuits. , 2016, , .		1
358	Open-loop temperature-compensated tuning of a 2-pole absorptive bandstop filter. , 2017, , .		1
359	Fully autonomous multiple-jammer suppression. , 2017, , .		1
360	Temperature-compensated open-loop tuning of a dual-notch absorptive bandstop filter. , 2017, , .		1

#	Article	IF	CITATIONS
361	An Inductor-based Real-time Monitoring and Control System for Tunable Cavity MEMS Filters. , 2018, , .		1
362	Efficient rectifier for wireless power transfer in VHF band. , 2018, , .		1
363	A New Reconfigurable Bandpass Filter With Adaptive Resonators for Switchable Passband and In-Band Notch. , 2019, , .		1
364	Assessing Students' Understanding of Solid-State Electronics in the First Introductory-Level ECE Course. , 2019, , .		1
365	High-Isolation Resistorless Tunable Filtering Power Divider. , 2020, , .		1
366	Microwave Wireless Powering of Sensored Agricultural Tile Drainages. IEEE Transactions on Antennas and Propagation, 2021, 69, 2913-2920.	3.1	1
367	An S-band Automatically Tunable Bandpass Filter Based on a Machine Learning Approach. , 2021, , .		1
368	Post-Release Displacement Uncertainty of Micro-Cantilevers Due to Anchor Over/Under Etching. , 2008, , .		1
369	A K-band Resonant Impedance Tuner with a Solid-State Hybrid Tuning. , 2022, , .		1
370	Planar reconfigurable slot antenna for communications. , 2001, , .		0
371	On-chip monopole antennas using pre-deformed cantilevers. , 2007, , .		0
372	Broadband tunable matching networks utilizing tapered lines. , 2007, , .		0
373	A variable beamwidth antenna for wireless mesh networks. , 2007, , .		0
374	MEMS liquid metal through-wafer microstrip to microstrip transition. , 2008, , .		0
375	CMOS-based monitoring of contact events up to 4 MHz in ohmic RF MEMS switches. , 2010, , .		0
376	Hermetically-sealed evanescent-mode resonators utilizing packaging as cavities. , 2010, , .		0
377	Corrections to "A Yagi–Uda Array of High-Efficiency Wire-Bond Antennas for On-Chip Radio Applications―[Dec 09 3315-3321]. IEEE Transactions on Microwave Theory and Techniques, 2011, 59, 1895-1895.	2.9	0
378	Tunable 3-D MEMS components for reconfigurable RF front-ends. , 2011, , .		0

#	Article	IF	CITATIONS
379	Remotely powered wireless strain telemeter. , 2011, , .		Ο
380	Radiation efficiency enhancement for dipoles placed adjacent to lossy silicon substrates. , 2012, , .		0
381	Real-time in situ electronic monitoring of dynamic contact behavior of MEMS high-g switches. , 2012, ,		0
382	Multi-point bearing cage wireless temperature sensor. , 2013, , .		0
383	Electromagnetic simulation of gas discharge effects in RF microgaps. , 2013, , .		0
384	The influence of gas discharge in nano-gap RF conductivity. , 2013, , .		0
385	(Invited) An X-Band Class-E Power Amplifier with MEMS Output Impedance Tuner. ECS Transactions, 2014, 60, 1121-1126.	0.3	0
386	Electromagnetic sensitivity analysis of RF gas micro/nano-breakdown. , 2014, , .		0
387	Magnetic nanoparticle ink for RF integrated inductor applications. , 2014, , .		0
388	Radio frequency gas breakdown and micro/nano-plasma formation in high-power evanescent-mode cavity resonators. , 2014, , .		0
389	IMS2014 Student Design Competitions. IEEE Microwave Magazine, 2014, 15, 56-58.	0.7	0
390	Development of 6-12 GHz evanescent-mode two-pole low-loss tunable bandpass filter. Microwave and Optical Technology Letters, 2015, 57, 2418-2422.	0.9	0
391	Reconfigurable filter design using resonators as coupling structures. , 2015, , .		0
392	Signal-interference RF wide-band bandpass filters using half-mode substrate-integrated-waveguide (HM SIW) directional couplers. , 2015, , .		0
393	Transient response enhancement of RF MEMS tuners using digital signal processing. , 2017, , .		0
394	Modeling inductance and quality factor of integrated spiral inductors on low-loss substrates up to 5 GHz. , 2017, , .		0
395	Low-temperature plasma for high-power tuning. , 2017, , .		0
396	Dark-to-Arc Transition in Air for Planar Electrodes with Microscale Gaps *. , 2017, , .		0

#	Article	IF	CITATIONS
397	Microwave-Driven CPW Microplasma Generator for Low-Power Discharge. , 2018, , .		0
398	High-Power and Widely-Tunable Evanescent-Mode Cavity-Backed Slot Antenna. , 2018, , .		0
399	Frequency-agile and spectrally sensitive radar transmitter amplifier optimizations. , 2018, , .		Ο
400	Evaluation of Electromagnetic Time Reversal Spatial Focusing (EMTR-SF). , 2019, , .		0
401	Electromagnetic Pulse Shaping and Applications. , 2007, , .		Ο
402	Analysis of Topographical Changes and Adhesion Failures in Gold-to-Gold Metal RF MEMS Switches With Cycling. , 2009, , .		0
403	Failure Analysis of Micron Scaled Silicon Under High Rate Tensile Loading. Conference Proceedings of the Society for Experimental Mechanics, 2014, , 157-158.	0.3	Ο
404	DESIGN CONSIDERATION OF LARGE-DISPLACEMENT RF MEMS TUNERS UNDER FABRICATION UNCERTAINTIES. , 2015, , .		0
405	Capacitive MEMS Switches. , 2016, , 425-437.		Ο
406	Miniaturization of Multi-Functional Filters Using Spiral Resonators Coupled to Their Scaled Negative Images. , 2022, , .		0